DEGRADATION OF LOAD-CARRYING CAPACITY OF STEEL I-GIRDER END DUE TO CORROSION

E. YAMAGUCHI*, and T. AKAGI

Department of Civil Engineering, Kyushu Institute of Technology, Kitakyushu, Japan

ABSTRACT

One of the crucial factors that could terminate the service life of a steel bridge is corrosion. Since many of the corrosion problems are found in the girder end, it is quite essential to know the load-carrying capacity of the girder end for efficient maintenance. To this end, the present study investigates the influence of corrosion at a girder end. Steel I-section girders with various corrosion models are constructed, and placing a vertical load at the upper flange right above the bearing, the girders are analyzed by nonlinear FEM. The degradation of the load-carrying capacity of a steel girder due to corrosion at its end is thus evaluated numerically. It is found that a different corrosion pattern at a girder end can lead to a significantly different degradation of the load-carrying capacity.

Keywords: Steel bridge, load-carrying capacity, girder end, corrosion.

1. INTRODUCTION

The maintenance of bridges is now a very important issue in Japan to keep a highway network in good condition, as the number of bridges started increasing rapidly in 1960s. As for the steel bridge, corrosion is one of the most influential phenomena on its service life: the corrosion could reduce the load-carrying capacity of the steel bridge, threaten its safety and eventually terminate its service. The cause for some 15% of the renewed highway steel bridges and some 50% of the renewed railway bridges is said to be corrosion (Hung et al. 2002).

Since the replacement of a bridge requires substantial cost, it is important to evaluate the load-carrying capacity of a corroded bridge for economic maintenance. Quite a few research studies indeed have been carried out, but much remains to be done, since corrosion patterns are numerous. In fact, the research is being continued: for example, the shear capacities of locally corroded steel I-section girders have been investigated and reported in 2011 (Liu et al. 2011).

The waterproof function of an expansion joint is quite susceptible to damage due to impact loads of moving vehicles. Therefore, water leakage from the expansion joint is often found, leading to the corrosion environment near the girder end. As a result, more corrosion problems occur near girder ends than in the other parts. Photo 1 shows an example. Clearly observed is the thinning of the transverse stiffener at the bearing.

* Corresponding author and presenter: Email: yamaguch@civil.kyutech.ac.jp

Photo 1: Corrosion of transverse stiffener.

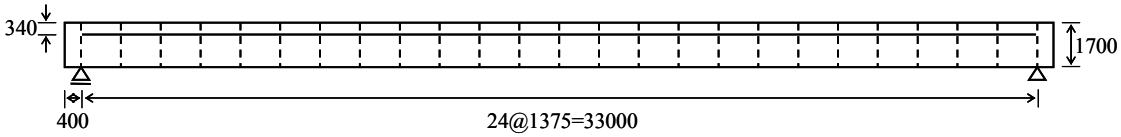

(a) Side view

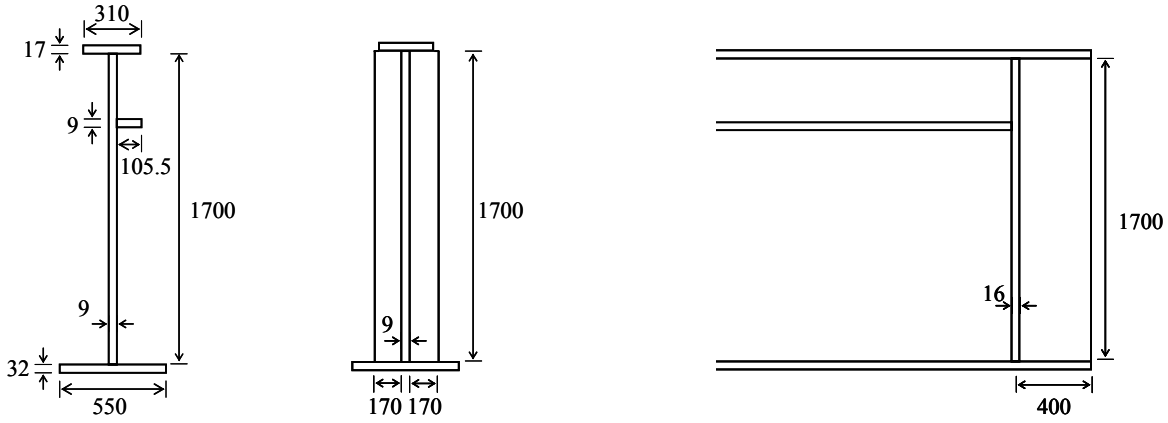

(b) Cross section of general part **(c) Cross section at bearing** **(d) Side view of girder end**

Figure 1: Steel I-section girder model (unit: mm).

The girder end is subjected to a concentrated load at the bottom, a reaction force from the bearing, and thus the degradation of the girder end could control the service life of a steel bridge. However, the number of studies on the load-carrying capacity of the girder end is quite limited and much remains to be done.

In the present study, the load-carrying capacity of a corroded steel girder end is investigated numerically. Various patterns of corrosion are considered, to this end.

2. STEEL I-GIRDER MODEL

Referring to a model bridge of Japan Bridge Association (2000), the steel I-section girder shown in Figure 1 is employed for the present study. Young's modulus E, Poisson's ratio and the yield stress are 2.0×10^5 N/mm^2, 0.3 and 235 N/mm^2, respectively. The nonlinear material behavior is assumed

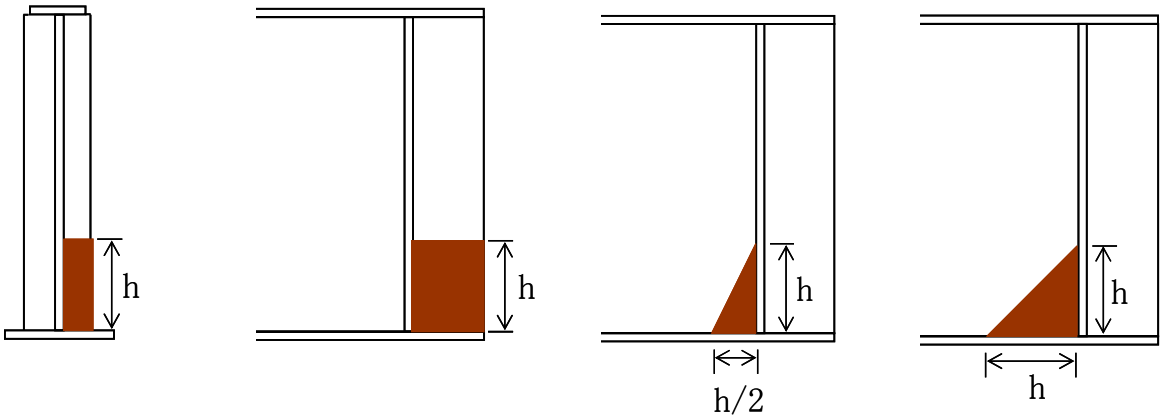

(a) CM-1S **(b) CM-1C** **(c) CM-1N** **(d) CM-1W**

Figure 2: Basic corrosion models.

to be described by the plasticity model of von Mises type. The associated flow rule and the kinematic hardening rule are applied. The uniaxial behavior is of bilinear type with the second slope $E/100$.

For the evaluation of the load-carrying capacity of a corroded girder, attention needs to be paid to the following:

(a) Local buckling in the corroded girder end above the bearing
(b) Shear buckling of the corroded web plate near the bearing
(c) Bending strength of the corroded girder

(a) is critical when a heavy truck runs above the bearing of the steel girder having a corroded girder end and has been studied by Huang et al. (2002). Following their investigation, (a), i.e. the load-carrying capacity of a corroded girder end, is studied also herein with more corrosion patterns included.

Using the design equation in Japan Road Association (2012), the design load-carrying capacity of the girder end of the present steel girder is found 1735 kN when it is not corroded.

3. CORROSION MODELS

Corrosion patterns have been investigated in several studies. For example, Huang et al. (2002) looked into the corrosion pattern of the steel girder very closely: a state of corrosion is more sever at the lower part of and on the inner surface of the girder.

Based on the observations available in literature, basic corrosion models are constructed in the present study. Those models are presented in Figure 2. Corrosion is assumed on one side of the girder.

The locations of CM-1S and CM-1C are in the transverse stiffener at the bearing and in the web of the cantilever part of the girder, respectively. The locations of CM-1N and CM-1W are both in the web, but the widths of the corrosion regions are different: CM-1W is twice as wide as CM-1N.

Only CM-1S is assumed to develop on the two surfaces of the transverse stiffener since the entire stiffener is on one side of the girder.

Combining the basic corrosion models, two corrosion models of CM-2N and CM-2W, are constructed. The former is the combination of CM-1S, CM-1C and CM-1N, while the latter CM-1S, CM-1C and CM-1W.

The corrosion models are grouped into two: the constituents of Group 1 are the basic models, while CM-2N and CM-2W constitute Group 2.

Various degrees of corrosion are considered: the height h and the plate-thickness loss on one side of a plate Δt are changed; 10%, 20% and 40% of the web height h_0 are given to h while Δt takes 2 mm, 4 mm and 6 mm. Δt is assumed uniform over each corroded region. Since corrosion develops on both surfaces of the transverse stiffener, the plate-thickness loss in the transverse stiffener is $2\Delta t$, twice as much as in the other corrosion models.

In the present study, thus 55 girders are to be analyzed, including the original (non-corroded) girder.

4. OUTLINE OF ANALYSIS

The load-carrying capacity of the steel I-section girder end is evaluated by finite element analysis with material and geometrical nonlinearies. Initial imperfections are also taken into account: the effects of residual stress and initial deflection are included in the analysis. To this end, the thermal stress analysis and the buckling analysis (eigenvalue analysis) are conducted in advance.

All the analyses are conducted by ABAQUS (2006). 4-node shell elements are employed. The load-carrying capacity of a girder end under loading above the bearing is the focus here. Deformation is expected to occur in a localized area above the bearing so that the area is modeled by finer elements. The girder is simply supported, but since it is analyzed in isolation, the horizontal movement of the upper flange is also restrained so as not to incur an inappropriate failure mode.

The localized deformation suggests that it may not be necessary to analyze the whole girder. Therefore, a quarter-length girder model is also constructed. Assuming no corrosion, analyses are conducted. The numerical results of the full girder model and the quarter girder model are shown in Figure 3. The two sets of the results are close to each other with the difference in the load-carrying capacity being 0.1%. In the following analyses, therefore the quarter model is to be used for saving computational cost. The finite element mesh of the quarter girder is presented in Figure 4.

5. NUMERICAL RESULTS

Figures 5-8 shows numerical results where P_{max} and P_0 are the load-carrying capacity of a corroded girder end and that of the non-corroded girder end. P_0 has been found 2542 kN (Figure 3).

With the increase of h and Δt, the load-carrying capacity decreases. Yet the way they influence the capacity varies from corrosion model to corrosion model.

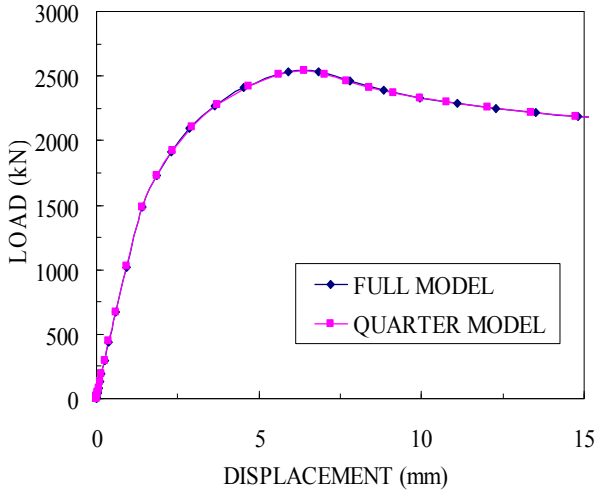

Figure 3: Load-displacement relationship at loading point.

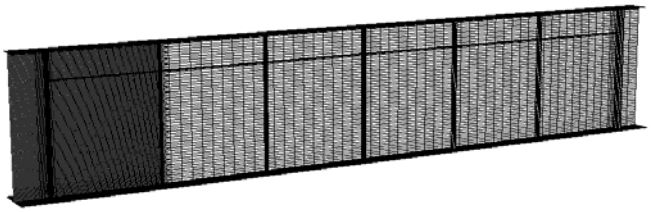

Figure 4: Finite element mesh of quarter girder model.

Figure 5 shows that for $h/h_0 = 0.1$, the load-carrying capacities of CM-1N and CM-1W barely decrease, even when Δt is large: the reductions are 0.1% and 0.2% for CM-1N and CM-1W, respectively, with $\Delta t = 6$ mm. In cases of CM-1S and CM-1C with $h/h_0 = 0.1$, the reductions in the load-carrying capacity of the girder end are very little up to $\Delta t = 2$ mm. But the capacity decreases as Δt increases: the reductions become 20% and 13% for CM-1S and CM-1C, respectively, with $\Delta t = 6$ mm. When h/h_0 is larger, the reductions in the load-carrying capacity are appreciable even with $\Delta t = 2$ mm: the reductions are 8% and 11% for CM-1S and CM-1C, respectively, when $h/h_0 = 0.4$.

The load-carrying capacity changes almost linearly with the increase of Δt except for CM-1S and CM-1C with $h/h_0 = 0.1$. However, even CM-1S and CM-1C with $h/h_0 = 0.1$ show the tendency of linear change between $\Delta t = 2$mm and $\Delta t = 6$ mm.

Figure 6 indicates that the increase of h/h_0 reduces the load-carrying capacity of the girder end. However, the capacity reduction is not linearly dependent on the increase of h/h_0. CM-1N and CM-1W show little degradation up to $h/h_0 = 0.1$. As h/h_0 increases, the load-carrying capacity tends to decrease significantly even in CM-1N and CM-1W. In case of CM-1S and CM-1C, the capacity reduction is small up to $h/h_0 = 0.1$ when $\Delta t = 2$ mm, while the capacity reduction is significant even between $h/h_0 = 0$ and 0.1 when $\Delta t = 4$ mm and 6 mm.

The average load-carrying capacity rate P_{max}/ P_0 of each corrosion model is found 0.855, 0.862, 0.966 and 0.945 for CM-1S, CM-1C, CM-1N and CM-1W, respectively. From this result, it can be stated that CM-1S has the largest influence while CM-1N the smallest. The difference between CM-1S and CM-1C and that between CM-1N and CM-1W are insignificant. But the influence of CM-1C is much larger than that of CM-1W. Thus the corrosion models can be classified into two groups in terms of the influence on the load-carrying capacity of a girder end: one group consists of CM-1S and CM-1C; the other consists of CM-1N and CM-1W. The corrosion regions in CM-1C

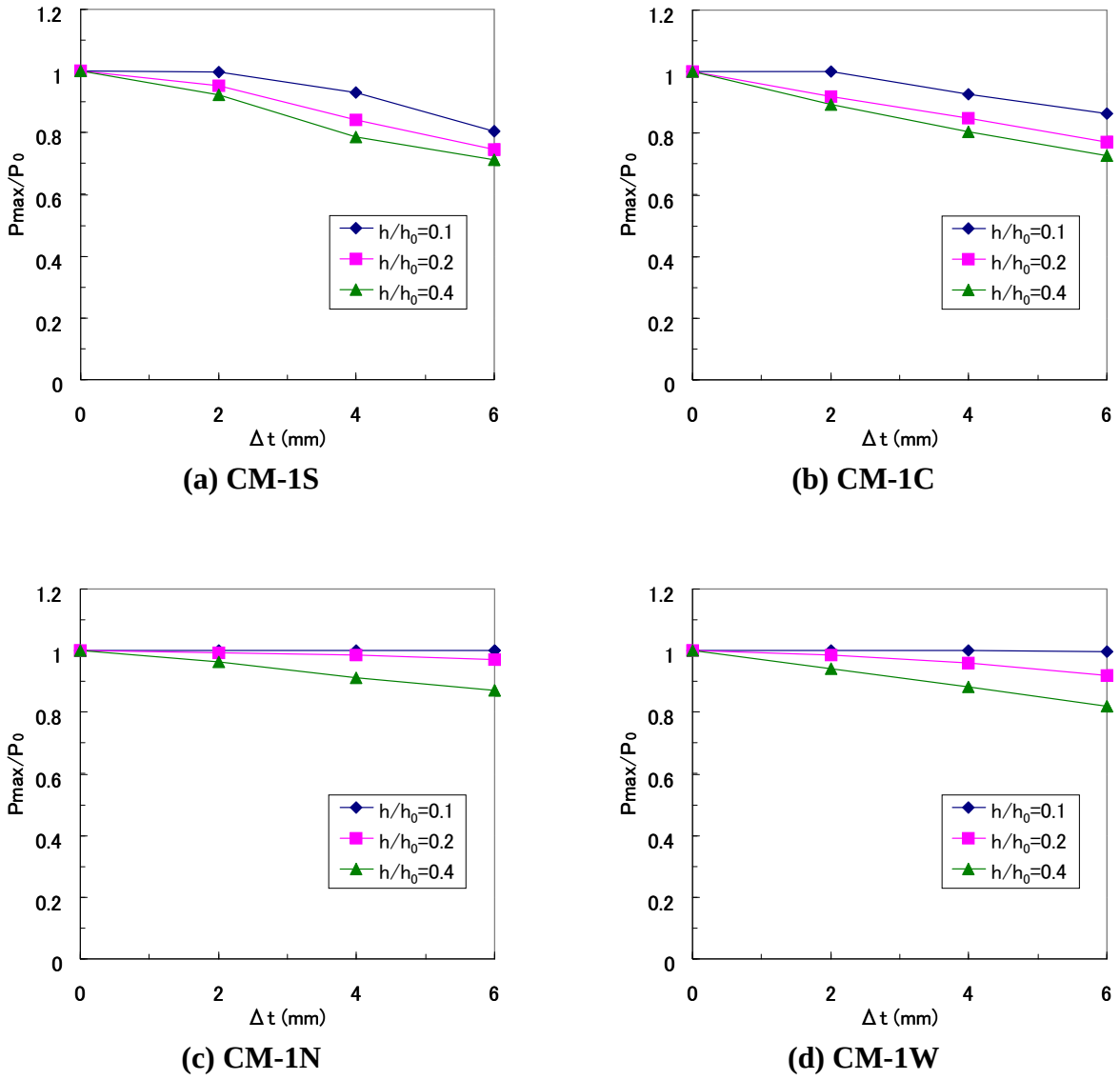

(a) CM-1S **(b) CM-1C**

(c) CM-1N **(d) CM-1W**

Figure 5: Variation of load-carrying capacity with plate-thickness loss (Group 1).

and CM-1S have a free boundary while CM-1N and CM-1W do not. The existence of the free boundary appears essential in discussing the degradation of the load-carrying capacity of a girder end.

Figures 7 and 8 are the results of Group 2. As expected, the reduction in the load-carrying capacity is much larger than in the case of Group 1. However, the way the load-carrying capacity changes are quite similar to that of Group 1: the load-carrying capacity varies almost linearly with the increase of Δt and the size of the corrosion in the web makes only a small difference.

In all the analyses, large deformation is observed in and around the corroded region. Obviously the failure mode is a sort of local buckling.

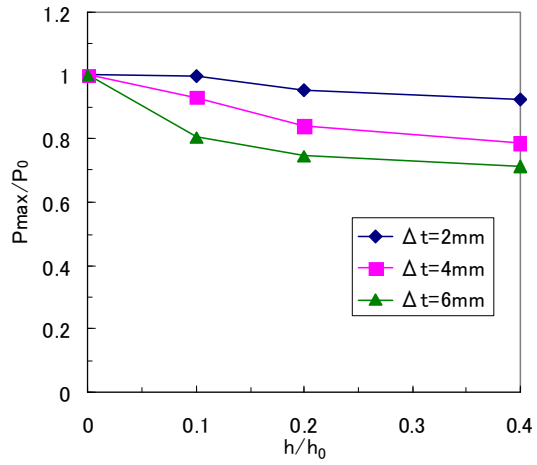

(a) CM-1S

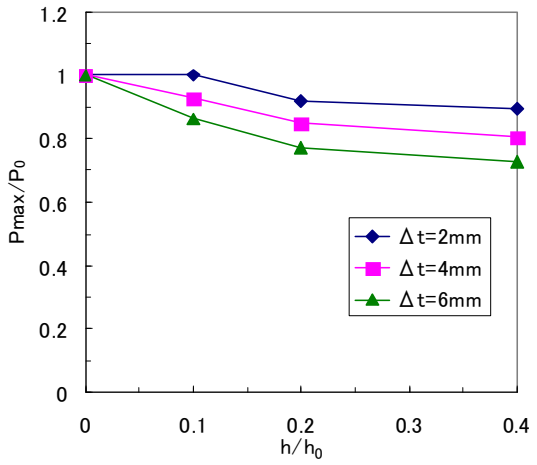

(b) CM-1C

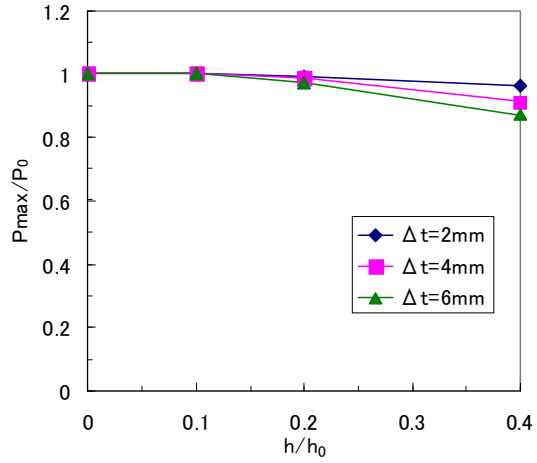

(c) CM-1N

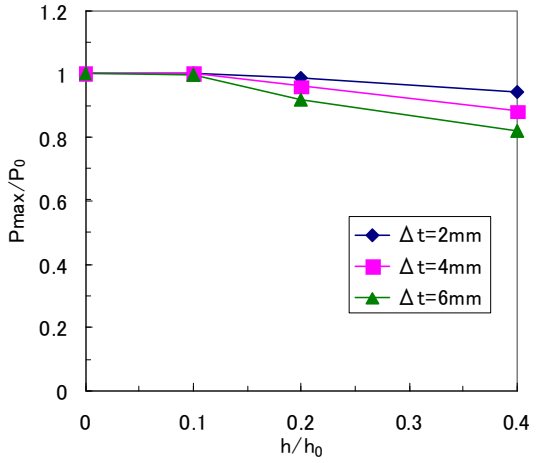

(d) CM-1W

Figure 6: Variation of load-carrying capacity with height of corroded region (Group 1).

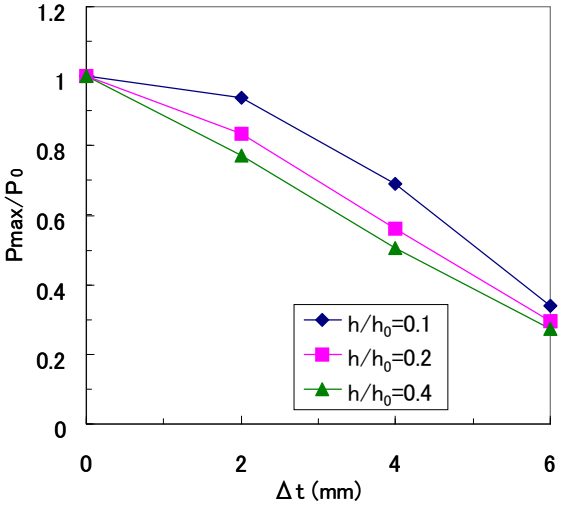

(a) CM-2N

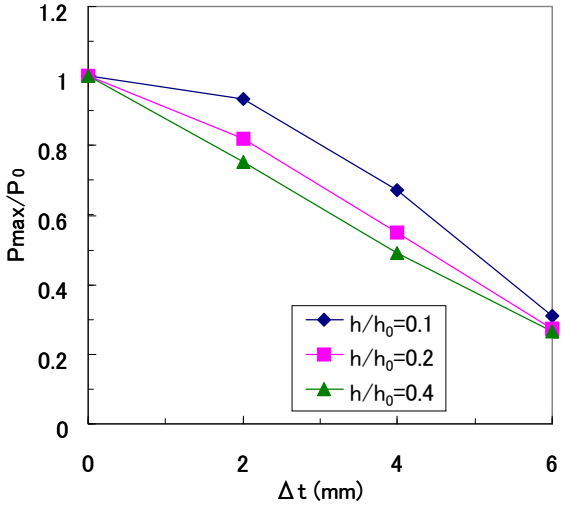

(b) CM-2W

Figure 7: Variation of load-carrying capacity with plate-thickness loss (Group 2).

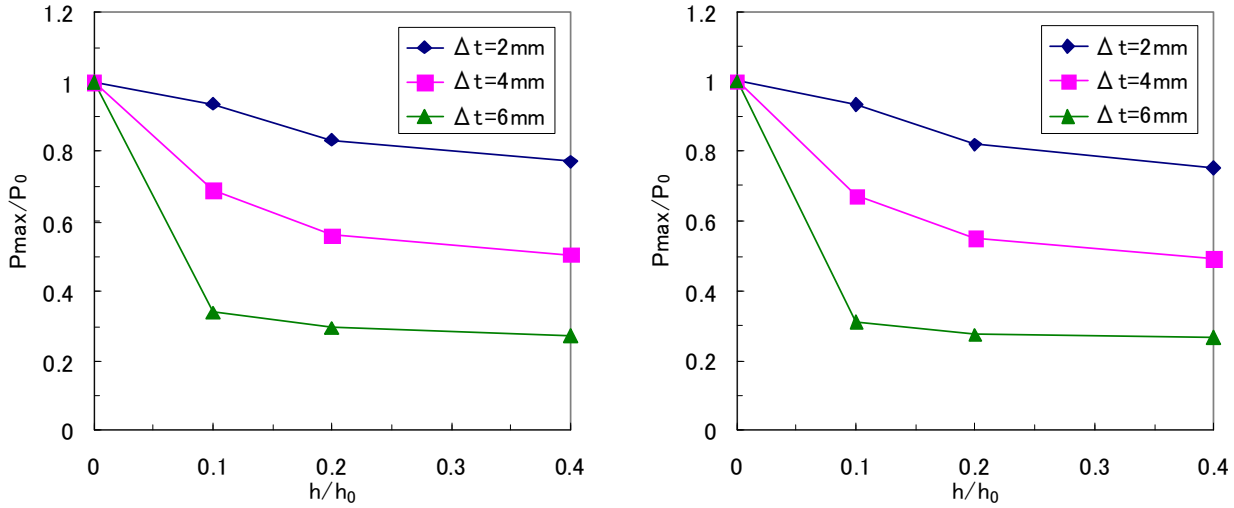

(a) CM-2N **(b) CM-2W**

Figure 8: Variation of load-carrying capacity with height of corroded region (Group 2).

6. CONCLUDING REMARKS

The present study reveals that the way corrosion influences the load-carrying capacity of a girder end depends on the location of corrosion. If the corroded region has a free boundary, the degradation of the load-carrying capacity of a girder end is large. The corrosion patterns considered herein, therefore, can be classified into two groups with respect to the degree of the degradation of the load-carrying capacity. It is also found that the load-carrying capacity of a girder end tends to decrease linearly with the increase of the plate-thickness loss.

The observations described above can give a general idea about the seriousness of corrosion in terms of the degradation of a girder end. If it is found significant, measure should be obtained such as the size of the corroded region and the plate-thickness loss as soon as possible and a careful safety evaluation needs be done.

7. ACKNOWLEDGMENTS

Financial support from the Japan Iron and Steel Federation for the present study is gratefully acknowledged.

REFERENCES

ABAQUS (2006). User's Manual. ABAQUS Ver. 6.6. Dassault Systemes Simulia Corp.

Hung, VT, Nagasawa, H., Sasaki, E., Ichikawa, A., and Natori, T. (2002). An experimental and analytical study on bearing capacity of supporting point in corroded steel bridges. Journal of JSCE. 710/I-60. pp. 141-151.

Japan Bridge Association (2000). Design Example and Explanation of Composite Girder.

Japan Road Association (2012). Specifications for Highway Bridges Part 2 Steel Bridges.

Liu, C., Miyashita, T., and Nagai, M. (2011). Analytical study on shear capacity of steel I-girder with local corrosion nearby girder ends. Journal of Structural Engineering, JSCE. 57A. pp. 715-723.